IV International Conference on Computational Methods for Coupled Problems in Science and Engineering
COUPLED PROBLEMS 2011
M. Papadrakakis, E. Oñate and B. Schrefler (Eds)

MULTIPHYSICAL COMPUTATIONS OF THE ELECTRICAL MACHINES USING FEM

A. STERMECKI [*†], O. BÍRÓ [*†], M. HETTEGGER[*†], H.LANG[♦], G. OFNER[♦], S. RAINER[†] AND B. WEILHARTER[●†]

[*]Institute for Fundamentals and Theory in Electrical Engineering (IGTE)
Graz University of Technology, Kopernikusgasse 24/3, 8010 Graz, Austria
e-mail: andrej.stermecki@tugraz.at, http://www.igte.tugraz.at

[●]Institute for Electrical Drives and Machines
Graz University of Technology, Inffeldgasse 18, 8010 Graz, Austria
e-mail: andrej.stermecki@tugraz.at, http://www.igte.tugraz.at

[†] Christian Doppler Laboratory for Multiphysical Simulation, Analysis and Design of Electrical Machines (MuSicEl)
Kopernikusgasse 24/3, 8010 Graz, Austria

[♦] ELIN Motoren Gmbh
8160 Preding/Weiz, Austria
e-mail: georg.ofner@elinmotoren.at, web page: http://www.elinmotoren.at

Key words: Acoustic noise, Electric machines, Electromagnetic forces, Multiphysics problems, Thermal analysis, Vibrations.

Abstract. In this paper three problems representing the multiphysical aspect of electrical machine computation are addressed. The interaction between magnetic and structural mechanical systems is demonstrated by the finite element method (FEM) structural investigation of the turbo-generator end-winding deformations. Multiphysical simulation of the acoustical problem is presented by weakly coupled electromagnetic, structural dynamic and acoustic simulations. And finally, a procedure based on computational fluid dynamics (CFD) simulation for acquiring the convective heat transfer coefficients is proposed in order to improve the accuracy of the coupled electro-thermal FEM simulations.

1 INTRODUCTION

In order to comply with modern demands for better efficiency and more environment-friendly machine-drives, they should be considered as comprehensive coupled systems, where effects of different physics are interacting with each other. The numerical computation of these phenomena is rather pretentious and often requires a substantial enhancement of the state of the art numerical procedures and highly efficient computing powers. In 2007 a new laboratory titled Christian Doppler Laboratory for Multiphysical Simulation, Analysis and Design of Electrical Machines (MuSicEl) has been established in the scope of the Institute for Fundamentals and Theory in Electrical Engineering (IGTE) and the Institute for Electrical

Drives and Machines of the Graz University of Technology. The research work of the laboratory is focused particularly on the development of efficient computational methods required for the consideration of the multiphysical nature of the electrical machines. In this paper three such representative electrical machine multiphysical problems are addressed in order to present the research activities of the Christian Doppler Laboratory for Multiphysical Simulation, Analysis and Design of Electrical Machines. The descriptions of the presented computational methods are based on the work published by the authors in [1], [2] and [3].

The investigation of the turbo-generator end-winding deformations shall demonstrate the interaction between magnetic and structural mechanical systems. The numerical approach based on the sequential coupling between a current-flow, an electromagnetic and a mechanical model is presented. In order to take the excitation produced by stator windings into consideration, a procedure based on coupled current flow and magnetic field analyses using dissimilar finite element (FE) meshes and numerical calculation of the Biot-Savart field has been employed. The magnetic forces acting on current conducting elements have been calculated and have been applied to the structural model. Under design operating conditions, computed harmonic forces specified by amplitude and phase have been applied to the mechanical model in order to simulate the frequency response of the end-winding system.

For the numerical computation of audible noise generated by induction machines, weakly coupled electromagnetic, structural dynamic and acoustic simulations have been accomplished [2], [4]. In order to comply with the different demands of each physical domain, different numerical formulations have been used for the simulation models besides applying different space discretizations. Electromagnetic excitation forces have been estimated by solving a transient nonlinear eddy current problem formulated by FE methods. The resulting forces have been applied to a linear structural dynamic FE model in the frequency domain. Finally, the acoustic sound pressure level is determined from the structural surface vibrations using the boundary element method.

Knowing the thermal boundary conditions is crucial in order to carry out coupled electrical-thermal analyses. The accuracy of the whole thermal simulation depends on the precision of those boundary conditions. Especially for complex geometries like the end-windings, there is no exact analytical method for the calculation of the convective heat transfer coefficient. A procedure based on computational fluid dynamics (CFD) simulation for acquiring the convective heat transfer coefficients is proposed.

2 ANALYSIS OF SYNCHRONOUS GENERATOR END-WINDING DEFORMATIONS

The structural investigation of synchronous machine end-region phenomena based on a numerical approach is an especially ambitious task, since the coupling of two models, each fitting different physics, needs to be accomplished. The numerical approach based on the sequential coupling between a current-flow, an electromagnetic and a mechanical model is presented in this paper. An electromagnetic simulation has been carried out in the frequency domain using a $\boldsymbol{T},\Phi$-Φ formulation [5]. The material nonlinearity has been taken into account by the employment of the effective $\boldsymbol{B}$-$\boldsymbol{H}$ curve [6]. The magnetic forces acting on current conducting elements have been calculated in the frequency domain and their time-varying

components have been applied to the structural model. A different FE mesh discretization of the mechanical model has been required in order to take into account the exact structural characteristics of the winding system and the construction parts.

2.1 Stator current excitation

Owing to the employed $\boldsymbol{T},\Phi$-Φ formulation [5], the current density in the stator three-phase winding ($\boldsymbol{J}$) needs to be represented by an arbitrary current vector potential $\boldsymbol{T}_0$ satisfying the following condition:

$$curl(\boldsymbol{T}_0) = \boldsymbol{J} \,. \tag{1}$$

One possible way to find an adequate function $\boldsymbol{T}_0$ is to calculate the Biot-Savart field produced by the stator current excitation. Static current flow analysis has been carried out in order to obtain the current distribution in the stator winding. Knowing the current distribution, the Biot-Savart field has been numerically computed in the integration points of another FE mesh representing the motor, its housing and the surrounding air. As seen in Fig. 1, the meshes of the stator winding and of the motor are non-conforming.

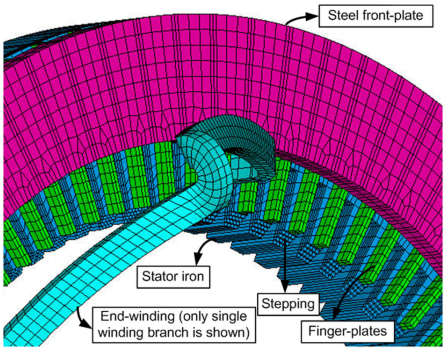

Figure 1. 3-D FE model of the motor and its end-winding.

The Biot-Savart field $\boldsymbol{H}_s$ has been evaluated for each phase excitation separately and by summing up the three magnetic field contributions, the complex representation of the rotating magnetic field intensity is obtained [1]. Knowing the numerically calculated Biot-Savart field, the rotational part $\boldsymbol{T}_0$ of the magnetic field is represented with the aid of edge element shape functions in order to avoid cancellation errors:

$$\underline{t}_i = \int_{\text{Edge } i} \underline{\boldsymbol{H}}_s \mathrm{d}l; \quad \underline{\boldsymbol{T}}_0 = \sum_{\text{Edge } i}^{n_e} \underline{t}_i \boldsymbol{N}_i \tag{2}$$

where N_i stands for the vectorial edge element shape functions associated with the i-th edge and ne for number of FE edges.

2.2 Rotor current excitation

The rotating magnetic field of the rotor is not generated by a 3-phase AC current excitation, but rather by DC currents and the mechanical rotation of the rotor making it impossible to be modeled in the same way as the stator excitation. In order to overcome this problem, a novel numerical method has been developed [1]. Using the $\boldsymbol{T},\Phi$-Φ formulation, the

rotor excitation has been defined by prescribing the rotating part $\boldsymbol{T}_0$ of the magnetic field in a thin finite element layer on the surface of the rotor [1]. It is sufficient to define the radial component of $\boldsymbol{T}_0$ only (Fig 3b), since this way the current density $\boldsymbol{J}$ in axial and azimuthal directions is taken into consideration:

$$curl\underline{\boldsymbol{T}}_0 = \frac{\partial \underline{T}_{0,r}}{\partial z}\boldsymbol{e}_\phi - \frac{1}{r}\frac{\partial \underline{T}_{0,r}}{\partial \phi}\boldsymbol{e}_z = \underline{\boldsymbol{J}} \tag{3}$$

where $\boldsymbol{T}_{0,r}$ denotes the radial component of the prescribed vector potential $\boldsymbol{T}_0$, $\boldsymbol{J}$ the current density in the rotor excitation winding and $\boldsymbol{e}_\phi$ and $\boldsymbol{e}_z$ the unit vectors in z and ϕ directions in a polar coordinate system. This way, the current excitations in axial and azimuthal directions are modeled in correspondence with the actual rotor winding distribution. In order to define the adequate amplitude of the prescribed potential $\boldsymbol{T}_0$ (3), the well known analytical expressions for the rotor current excitation have been taken into consideration. The detailed description of this procedure can be find in [1]. Knowing the distribution of the magnetic field, the Lorentz forces acting on the stator end-winding have been calculated. Since the computation has been carried out in the frequency domain, the constant as well as the oscillating parts of the forces have been evaluated. The latter forces oscillating with double nominal frequency (100 Hz) are especially important for the structural investigations of the nominal operating conditions. Therefore, these forces have been used as an input for the structural mechanical analysis carried out in the next step.

2.3 Structural mechanical analysis

Another FE mesh has been used for the structural harmonic analysis. A detailed mechanical structure consisting of winding bars, poromat bricks, fabric tubes, cantilevers, finger-plates and the stator package has been modeled. Since non-conforming meshes have been used for all parts, contact elements have been employed to link the different parts. A separate pre-processor program has been developed in order to parametrically define the model's geometry and to obtain a finite element mesh composed of well shaped hexahedron elements. Finally, the investigation of the structural behavior has been carried out in the program package ANSYS [7].

The final goal of the presented mechanical investigations has been to determine deformations of the end-winding system caused by the calculated excitation. The extent of the resulting deformations can be attributed to individual deformation waves of different ordinal numbers. In order to avoid mechanical resonances, the lowest natural frequency of the end-winding system has to be located distant enough from the excitation frequency. It is safe to assume that, for the machine under research, all natural frequencies above 140 Hz are not going to be highly stimulated by the excitation frequency of 100 Hz. The natural frequencies have been ascertained by performing a modal analysis. Moreover, a harmonic analysis has been carried out as well in order to compute the exact deformations due to the force excitation.

2.4 Results

In the present work, a crucial impact of the boundary conditions on the calculated winding forces has been ascertained. In order to compute the magnetic field as accurately as possible,

the problem has been solved in the frequency domain and eddy currents induced in the housing, the bearing shield, the clamping-fingers and the clamping-plate have been taken into consideration. In Fig. 2a the eddy currents in the portion of the steel clamping-plate and the front clamping-fingers are shown.

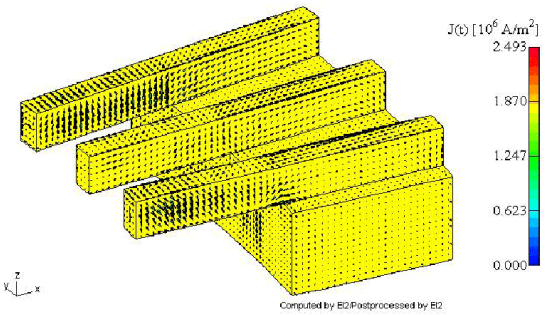

Figure. 2a. Induced eddy currents in the clamping -plate and –fingers.

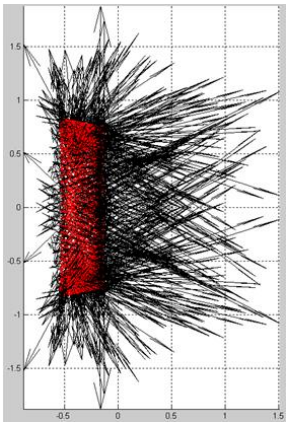

Figure. 2b. Side view of the forces acting on stator end-windings.

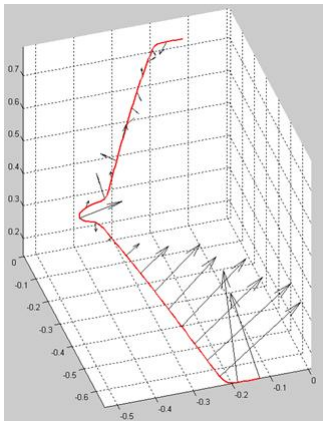

Figure. 2c. Forces acting on a single stator winding branch.

In Fig. 2b, the oscillating parts of the forces acting on the stator end-winding are shown. As seen from the Fig. 2b, the forces are symmetrically distributed over 72 stator slots and maximal force densities are obtained at the positions near the rotor package (Fig. 2c).

The results of the harmonic analysis are given in Fig. 3. Outcomes of two methods are presented and mutually compared. The deformations shown in Fig. 3a have been obtained by full stiffness and mass matrices. The modal superposition method taking into consideration the first twenty modes only has been used to obtain the deformations shown in Fig. 3b. Based on the presented results (Fig. 3), the conclusion can be drawn that all essential deformation characteristics are kept even when a less complex and less time-consuming modal superposition method is employed.

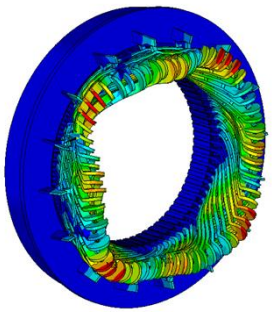

Figure. 3a. End-winding deformations (harmonic analysis using full mass and stiffness matrices).

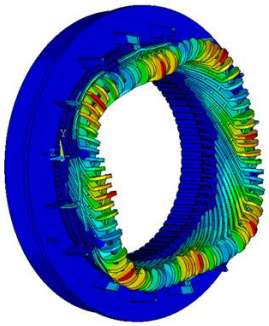

Figure. 3b. End-winding deformations (harmonic analysis using modal superposition of the first 20 modes).

The proposed method is very time-efficient, since a transient time-stepping analysis has

been avoided, which would otherwise be required to consider the rotor excitation. It has to be mentioned that the rotor slots harmonics have been neglected in this procedure, since only the fundamental spatial harmonic of the prescribed vector potential to the rotor has been taken into consideration. Nevertheless, a further improvement of this method is possible by imposing the excitation fields of higher-order harmonics to the FE layer on the rotor surface.

The proposed procedure has been employed to investigate the structural behavior of a synchronous generator. The findings of this study lead to a conclusion that, for the machine under research, the natural frequencies of the end-winding are not interfering with the excitation frequency. Consequently, the obtained deformations by harmonic analysis are also within the expected μm range and no negative influences on the end-winding life-cycle are to be expected. These simulation results have also been confirmed by the measurement results.

3 NUMERICAL COMPUTATION OF THE NOISE RADIATION OF AN INDUCTION MACHINE

The reasons for audible noise generated by electrical machines are, besides mechanical causes, as for example bearings, brush noise or rotor unbalance, and noise of aerodynamic origin, certain aspects in the electromagnetic field generation [8], [9]. Due to the permeance fluctuations, e.g. arising from the slotting or saturation effects, and the winding composition, the magnetic flux distribution in the airgap contains, apart from the fundamental wave, time-harmonics of higher order. Due to the electromagnatic field in the airgap, forces with according harmonics acting on the rotor and stator surface occur. Obviously, the electromagnetic forces acting on the stator lead to its deformation and thus also the deformation of the housing. The resulting vibrations result in pressure fluctuations of the enclosing air and thus audible noise is generated. Therefore, for computations of audible noise with electromagnetic origin, three different physics, namely electromagnetics, mechanics and acoustics, have to be considered and coupled accordingly. A comprehensive numerical approach shall be presented in this paper. A detailed version of this approach can be found in [2].

3.1 Electromagnetic Field Computation

The electromagnetic field in the airgap, with the magnetic flux density B, results in the mechanical stress σ, which can be computed in time domain according to [10] with the following relation

$$\sigma_n = \frac{1}{2\mu_0}(B_n^2 - B_t^2) \tag{4}$$

$$\sigma_t = \frac{1}{\mu_0} B_n B_t , \tag{5}$$

where μ_0 denotes the magnetic permeability for vacuum and the indices n and t the normal and tangential component of the magnetic flux density B. The determination of B is carried out numerically with a finite element multi-slice simulation [11], which also enables the consideration of skewing effects. The axial dimension is divided into five slices which are represented by two dimensional finite element models. These models, more precisely the

currents in the rotor bars, are then connected via an electric circuit. The $A, v-A$ formulation [12] is used to solve the nonlinear and transient eddy current problem. The solution yields results for the magnetic flux density B in the airgap at distinct axial positions. For the successive structural computation the stress distribution in the airgap along the axial dimension is needed. Hence the axial characteristic of B has to be reconstructed from the multi-slice simulation results. Therefore the time-harmonics and spatial harmonics of the magnetic flux density B, implying a 2D Fourier transformation, are needed. The spatial order in axial direction is computed analytically and a correlation with the harmonics of the multi-slice solution enables the reconstruction, see [13]. The mechanical stress acting on the teeth of the stator can now be computed according to (4) and (5) in time domain.

3.2 Structural Vibration Computation

To determine the structural vibrations the finite element method is used. A three-dimensional model of the investigated machine, comprising the main parts stator, rotor, windings and housing, has to be set up and discretized appropriately. As only the steady state solution is of interest, the simulation can be performed in frequency domain. According to [14], the dynamical behaviour of the structure for the excitation frequency Ω is therefore described by

$$(-\Omega^2\mathbf{M}+\mathbf{K})\underline{\hat{\mathbf{x}}}=\underline{\hat{\mathbf{F}}} \tag{6}$$

with the mass matrix $\mathbf{M}$ and the stiffness matrix $\mathbf{K}$. $\underline{\hat{\mathbf{F}}}$ and $\underline{\hat{\mathbf{x}}}$ denote the complex nodal force amplitude and the complex deformation amplitude for the excitation frequency Ω. It is assumed that the deformation does not influence the magnetic flux distribution, which results in a weakly coupled problem. The mechanical stress σ has to be transformed into frequency domain, or directly computed in this domain. The nodal forces at the excitation frequencies can then be determined and impressed onto the structural model. Solving (6) then provides the deformation characteristic on the surface of the machine, which is of interest for the noise computation.

3.3 Acoustic Computation

To determine, in a last step, the noise radiation due to the machine vibrations and surface oscillations the homogeneous Helmholtz equation

$$\Delta p + k^2 p = 0 \tag{7}$$

with the wave number k has to be solved, regarding the sound pressure p, for an exterior radiation problem. Therefore the Sommerfeld radiation condition

$$\lim_{R\to\infty}\left[R\frac{\partial p}{\partial R}-jkp\right]=0 \tag{8}$$

with R denoting the radial distance, has to be satisfied, meaning that any acoustic disturbance caused by the structure dies out at infinity.

To solve (7) the boundary element method [15], [16] is used. Only the surface of the investigated structure has to be discretized and furthermore (8) is fulfilled implicitly when using this method, which are great advantages compared to the finite element method. From the structural frequency domain solution for the deformation $\underline{\hat{\mathbf{x}}}$ the velocity of the surface vibration can be computed. Again the influence of the sound pressure on the structural deformation is neglected and thus weak coupling is assumed. The normal components of the

velocity are applied to the surface elements as a boundary condition for the boundary element problem. The solution of the Neumann problem of (7) is the sound pressure on the surface of the investigated machine. To get the sound pressure distribution in the circumference of the investigated structure a field, where the boundary element solution is evaluated, discretized with appropriate elements, has to be set up.

3.4 Numerical Simulation Results

The numerical simulation has been carried out for an induction machine with a cylindrical cooling jacket. The rotor is skewed for one stator slot pitch and has a speed of 2991 rpm at nominal operating point. Acoustic measurement showed a noise peak at 1895.6 Hz of approximately 78 dB. The solution of the transient electromagnetic simulation shows a time harmonic of the surface stress occurring at this frequency. In Fig. 4a the computed real part of the radial component of the mechanical stress acting on the stator teeth is depicted.

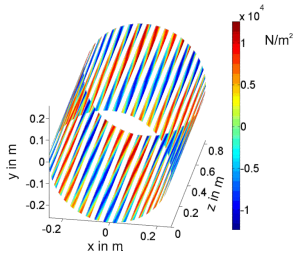

Figure. 4a. Teeth forces in radial direction

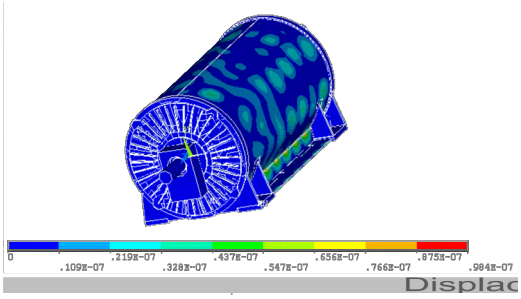

Figure. 4b. Real part displacement solution

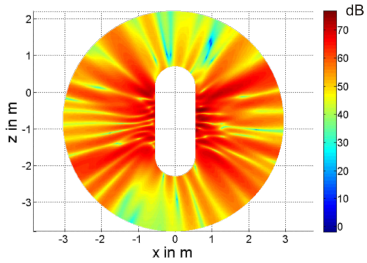

Figure. 4c. Sound pressure level on a plane field surrounding the machine

This resulting stress distribution is impressed on the mechanical finite element model and the structural deformation is computed according to (6). The solution is shown in Fig. 4b. It can be seen that the deformation characteristic is dominated by plate bending, which can be lead back to the eigenmodes near the excitation frequency. This plate bending causes the pressure fluctuations in the air and thus the radiating noise. The sound pressure level in a horizontal plane field, passing through the rotation axis of the rotor, is depicted in Fig. 4c. The main part of the noise is radiating from the cylindrical surfaces, as there the highest deformation amplitudes occur. The sound pressure level of more than 70 dB near the machine's surface is decreasing with the distance. At a surrounding sphere maximal sound pressure levels of approximately 70 dB can be detected. This however deviates from measurement results which yield approximately 78 dB at the excitation frequency and in 1 m distance for this induction machine. The deviations can be explained by the lack of validated material parameters for the structural model and by the possible influence of the forces acting on the rotor core stack.

4 DETERMINATION OF CONVECTIVE HEAT TRANSFER COEFFICIENT AT END WINDINGS FOR TEMPERATURE FIELD SIMULATIONS

The transport of thermal energy can be split into three different physical phenomena heat radiation, heat conductance and heat convection. All three of these phenomena can occur at the same time and can be cumulated into the total heat flux $\dot{q}_{tot}$.

Under common operating conditions of electrical machines the heat radiation transports a negligible portion of thermal energy. Due to its dependency on the fourth power of the temperature difference its influence on the total energy balance is rarely perceptible. For a simple test case of a radiating body in a free environment the heat radiation can be written as

$$\dot{q}_{rad} = \varepsilon\sigma \cdot (T^4 - T_\infty^4), \tag{9}$$

where ε is the emissivity, σ the Stefan-Boltzmann constant and T_∞ denotes the ambient temperature. Nevertheless it should not be discarded completely from the design process of electrical machines. In certain situations the heat radiation can be an observable fact, for instance for machine types, which allow higher temperatures at the housings surface. In this case the magnitude of heat flux by radiation can reach the value of heat flux by free convection, and must be considered [17].

The procedure of conductive heat flow simulation in solid materials is well known and reliable. The distribution of temperature inside the material can be solved for instance with finite element method (FEM) by solving the Laplace equation

$$\dot{q}_{cond} = -\lambda \cdot \nabla T \tag{10}$$

with the conductive heat flux $\dot{q}_{cond}$. A homogenisation of the material properties [17] can simplify the computation model [3] for components with non isotropic thermal conductivity λ like laminated iron sheets and insulated copper windings. At contact regions of different solid materials or a thin layers of a different substances a special treatment of the FEM model is necessary, in order to avoid a very fine resolution of the mesh. In these cases the application of certain element types can include these effects as proposed in [18]. Its accuracy satisfies most requests of engineering purposes if proper boundary conditions have been specified.

The boundary to the adjoining fluid coolant is specified by the convective heat flux

$$\dot{q}_{conv} = \alpha \cdot (T - T_\infty) \tag{11}$$

with the convective heat transfer coefficient α. This convective heat transfer coefficient depends basically on the fluid properties of the coolant and its flow conditions like velocity and turbulence. In general α can be defined for certain areas or locally α_x for certain points at the surface. If the heat transfer coefficient is defined locally one has to take under consideration the validity of its value. Due to its definition with the environmental temperature T_∞ it can be physically invalid if the difference between surface temperature and environmental temperature becomes zero but the convective heat flux $\dot{q}_{conv}$ does not [19].

The convective heat transfer coefficient can be derived analytically only for very simple geometries in the case of laminar flow conditions. In the case of turbulent flow conditions at complex geometries with rough surfaces only empirical approaches could be used in the past. Due to the improvements of computational fluid dynamics (CFD) and the nowadays available

computational power, it is possible to derive the convective heat transfer coefficients of any geometry numerically. An exact derivation of the convective heat transfer can be done with direct numerical simulation (DNS) but it requires a mesh resolution based on the Kolmogorov length scale η

$$\eta = \left(\frac{\nu^3}{\varepsilon} \right)^{1/4}, \tag{12}$$

which is defined by the kinematic viscosity ν and the turbulence dissipation rate ε. By using this length scale the element size of the mesh has to be in the magnitude of several micrometers for an electric machine**,** which uses air as cooling fluid. Hence this dramatically enlarges the number of elements and degrees of freedom, thus DNS is not a suitable method for industrial applications. Models which are based on eddy viscosity are more appropriate for engineering purposes and should be used instead DNS. Hence these numerical simulation models are based on certain simplifications, they can not be used for all kind of flow conditions in the same way and can fail in calculating the heat transfer. Therefore it is still necessary to validate the derived results by measurements or other empirical approaches. Especially at low velocities and thus low Reynolds numbers certain turbulence models fail in predicting the heat flux at the surface. The occurrence of flow separation and reattachment of the fluid cannot always be predicted accurately but it makes a crucial difference in the derivation of the heat transfer.

According to the investigations in [20] and [21] the Shear Stress Transport (SST) turbulence model [22] and the Scale Adaptive Simulation (SAS) turbulence model [23] meets the requirements for the prediction of the heat transfer coefficient best.

In Fig. 5 the derived heat transfer coefficient is shown related to its maximum.

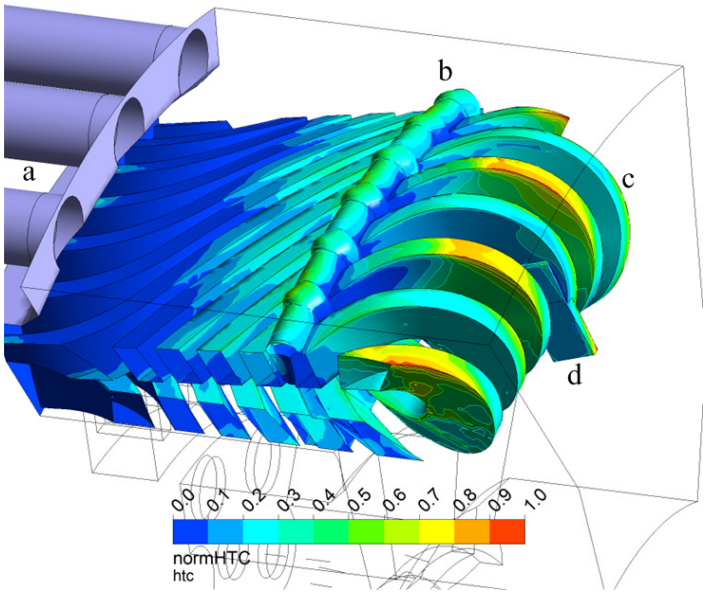

Figure 5: Norm values of the local heat transfer coefficient at the surface of the end-windings of an induction machine, with the cooling ducts (a), cord (b), end windings (c) and a heat flux sensor (d) which has been meshed with the end-windings' geometry in order to validate the simulation results.

As one can see, the heat flux reaches the maximal value at the outermost position of the end-windings**,** where the conductors are exposed directly to the air flow from the cooling ducts. The results shown in Fig. 5 have been derived by the use of the SAS turbulence model, using constant values for the temperature at the models' surfaces and temperature dependent fluid properties as used in [24].

These derived values for the local heat transfer coefficient can be used for the simulation of the temperature distribution inside the solid material of the electric machine. This should lead to more accurate results than using mean values for the convective heat transfer coefficient.

ACKNOWLEDGMENT

This work has been supported by the Christian Doppler Research Association (CDG), by the ELIN Motoren Gmbh and Traktionssysteme Austria GmbH.

REFERENCES

[1] A. Stermecki, O. Bíró, G. Ofner, and H. Lang, "*Numerical Simulation of Electromagnetic Phenomena in Motor End-Regions*", e & i Elektrotechnik und Informationstechnik, submitted for publication.

[2] BG. Weilharter, O. Bíró, H. Lang and S. Rainer, "Computation *of the Noise Radiation of an Induction Machine Using 3D FEM/BEM*", COMPEL, submitted for publication.

[3] M. Hettegger, O. Bíró, A. Stermecki, G. Ofner, "*Temperature rise determination of an induction motor under blocked rotor conditions*", PEMD 2010, Brighton 2010.

[4] B. Weilharter, O. Bíró, H. Lang, G. Ofner and S. Rainer, "*Validation of a Comprehensive Analytic Approach to Determine the Noise Behaviour of Induction Machines*", ICEM 2010, Rome 2010.

[5] O. Bíró, K. Preis, G. Vrisk, K. R. Richter and I. Ticar, "*Computation of 3-D Magnetostatic Fields Using a Reduced Scalar Potential,*" IEEE Transaction on Magnetics, 29(2): 1329-1332, 1993.

[6] G. Paoli, O. Biro, and G. Buchgraber, "*Complex Representation in Nonlinear Time Harmonic Eddy Current Problems*," IEEE Transaction on Magnetics, vol.34, no.5, pp.2625-2628, September 1998.

[7] *ANSYS 11.0 documentation* (2007). SAS IP, Canonsburg.

[8] P. L. Timar, *Noise and Vibration of Electrical Machines*, Elsevier, 1989.

[9] H. Jordan, *Der geräuscharme Elektromotor*, W. Girardet, 1950.

[10] J. Melcher, *Continuum Electromechanics*, MIT Press, Cambridge, MA, 1981.

[11] P. Dziwniel, B. Boualem, F. Piriou, J.P. Ducreux and P. Thomas, "*Comparison Between Two Approaches to Model Induction Machines with Skewed Slots*", IEEE Transactions on Magnetics, vol. 36, no. 4, pp. 1453-1457, 2000.

[12] O. Bíró, "*Edge element formulation of eddy current problems*", Comput. Methods Appl. Mesh. Engrg., vol 169, no. 3, pp 391-405, 1999.

[13] B. Weilharter, O. Bíró and S. Rainer, "*Computation of rotating force waves in induction machines using multi-slice models*", IEEE Transactions on Magnetics, submitted for publication.

[14] K. J. Bathe, *Finite Element Methods*, Springer.

[15] R.D. Ciskowski and C. A. Brebbia, *Boundary Element Methods in Acoustics*, Computational Mechanics Publications, Elsevier Applied Science.

[16] Y. J. Liu and F. J. Rizzo, "*Hypersingular boundary integral equations for radiation and scattering of elastic waves in three dimensions*", Computer Methods in Applied Mechanics and Engineering, vol. 107, pp. 131-144, 1993.

[17] Richter, R. *Elektrische Maschinen* Springer, 1967, XVI, 691 Seiten.

[18] Driesen, J.; Belmans, R. & Hameyer, K. *Finite-element modeling of thermal contact resistances and insulation layers in electrical machines Industry Applications*, IEEE Transactions on DOI - 10.1109/28.903121, Industry Applications, IEEE Transactions on, 2001, 37, 15-20.

[19] Herwig, H. *Kritische Anmerkungen zu einem weitverbreiteten Konzept: der Wärmeübergangskoeffizient α* Forschung im Ingenieurwesen, Springer Berlin / Heidelberg, 1997, 63, 13-17.

[20] Hettegger, M.; Streibl, B.; Biro, O. & Neudorfer, H. "*Identifying the heat transfer coefficients on the end-windings of an electrical machine by measurements and simulations"*, Electrical Machines (ICEM), 2010 XIX International Conference on DOI - 10.1109/ICELMACH.2010.5608250, 2010, 1-5.

[21] Hettegger, M.; Streibl, B.; Biro, O. & Neudorfer, H. "*Measurements and Simulations of the Heat Transfer on End Windings of an Induction Machine*", 14th International IGTE Symposium, 2010, 23 - 23.

[22] Menter, F. R. "*Two-Equation Eddy-Viscosity Turbulence Models for Engineering Applications",* AIAA Journal, 1994, 32, 1598-1605.

[23] Egorov, Y. & Menter, F. "*Development and Application of SST-SAS Turbulence model in the DESIDER Project"*, CFX Technical Memorandum, 2007, CFX-VAL10/0602.

[24] Hettegger, M.; Streibl, B.; Biro, O. & Neudorfer, H. "*Characterizing the heat transfer on the end-windings of an electrical machine for transient simulations*", MELECON 2010 - 2010 15th IEEE Mediterranean Electrotechnical Conference DOI - 10.1109/MELCON.2010.5476025, 2010, 581-586.